Self-templated nanotubes

DOI: 10.1002/smll.200700105

Self-Templated Growth of Carbon-Nanotube Walls at High Temperatures**

Jian-Yu Huang, Feng Ding, Kun Jiao, and Boris I. Yakobson*

Carbon nanotubes posses many remarkable properties and hold numerous potential applications.[1–15] However, the growth mechanisms, in particular, the noncatalytic growth of nanotubes, remains unclear, which poses fundamental difficulties in tailoring their structure for specific applications. For the noncatalytic growth of nanotubes, such as the arc discharge and laser ablation methods, three types of mechanism have been proposed, categorized as gas, solid, and liquid mechanisms.[16–22] The gas-phase models assume that nanotubes nucleate and grow directly from the vapor. In solid-phase models, the nanotubes are crystallized from an amorphous precursor, while the liquid-phase model suggests that nanotubes crystallize from liquid carbon. There is currently no agreement about which of these mechanisms is correct. All of the previous proposed noncatalytic growth mechanisms are mainly based on the observation of the post-grown nanotubes. In situ observation of noncatalytic nanotube growth remains a challenge. Here we report an in situ atomic-scale observation of a noncatalytic layer-by-layer self-templated assembly of carbon-nanotube walls at high temperature induced by high-bias Joule heating. The self-templated growth results in the thickening of the nanotube walls and an increase in electrical conductivity. High-temperature annealing is therefore an effective method to improve the structural quality and the electrical properties of nanotubes. In situ observation of the structural changes of nanotubes during Joule heating at high temperatures can provide an effective way to reveal the growth mechanism of carbon nanotubes.

Our experiments were carried out in a JEOL 2010F high-resolution transmission electron microscope (HRTEM) equipped with a Nanofactory TEM-STM (scanning tunneling microscopy) platform.[23–28] Multi-walled carbon nanotubes (MWCNTs) synthesized by chemical vapor deposition (CVD) were first attached to a gold rod with diameter of about 250 μm by using a conductive glue, and then individual MWCNTs protruding from the gold rod were approached and bonded to the STM tip by electron-beam deposition of amorphous carbon (Figure 1a–b) inside the HRTEM. A high current was passed through the nanotube to Joule heat it to temperatures higher than 2000 °C.[23–28] At such high temperatures, a layer-by-layer self-templated growth of nanotube walls occurred.

Figure 1b shows a MWCNT, the surface of which is coated with amorphous carbon. The MWCNT is bent due to pushing of the STM probe. When a bias voltage of 2.3 V was applied to the nanotube, electric breakdown[23–32] occurred in the right section of the nanotube (Figure 1c). The length of the breakdown segment is about 40 nm. The nanotube diameter is usually not uniform because of the different thickness of amorphous coating, and the breakdown usually occurs at the thinnest segment or the most defective sites in the nanotube.[23–28] The electric breakdown washed out most of the amorphous carbon on the surface of the breakdown section of the nanotube. In the mean time, the amorphous carbon on the other part of the nanotube surface crystallized into curved and poorly organized graphite layers. The electric breakdown created a clean surface, which is best suited for in situ structural observations. After maintaining a constant bias voltage of 2.3 V for about 2 h, the number of walls of the nanotube increased from the initial 32 shells (Figure 1d) to the final 50 shells (Figure 1e). Interestingly, the nanotube hollow (Figure 1b and d) in the breakdown segment disappeared after the wall growth (Figure 1c and e). With increasing number of walls, the current flowing in the nanotube was increased continuously from 370 to 470 μA (Figure 1f), and the low bias conductance was increased from 0.8 G_0 to 1.5 G_0 ($G_0 = 12.9$ kΩ is a quantum conductance).

In situ microstructure investigations indicated that the thickening of the MWCNTs (Figure 1e) was attributed to a layer-by-layer self-templated growth mechanism, as shown in Figures 2 to 6. The self-templated growth occurred in both the inner (Figure 2) and the outer surfaces (Figures 3–6) of the nanotubes. The HRTEM images shown in Figures 3 to 6 were all taken from the breakdown section of the same nanotube as shown in Figure 1. Because the nanotube is too thick, only part of the walls were shown in Figures 3 to 6.

Interestingly all the disordered carbon structures such as carbon onions and incomplete graphene layers (Figure 1b and d) inside the MWCNTs were totally transformed to the inner layers of the MWCNT (Figure 1c and e). The hollow space inside the MWCNT completely disappeared after the high temperature treatment (Figure 1d), which was attributed to the growth of new nanotube walls in the inner surface.

[*] Dr. J.-Y. Huang
Center for Integrated Nanotechnologies (CINT)
Sandia National Laboratories
Albuquerque, NM 87185 (USA)
Fax: (+1) 505-284-8478
E-mail: jhuang@sandia.gov
Dr. F. Ding, K. Jiao, Prof. B. I. Yakobson
Department of Mechanical Engineering and Materials Science
and
Department of Chemistry, Rice University
Houston, TX 77005 (USA)

[**] This work was supported in part by the Center for Integrated Nanotechnologies, the U.S. Department of Energy, the Office of Basic Energy Sciences user facility, and in part by Laboratory-Directed Research and Development (LDRD). Sandia is a multiprogram laboratory operated by Sandia Corporation, a Lockheed Martin Company, for the United States Department of Energy's National Nuclear Security Administration under Contract DE-AC04-94AL85000. Work at Rice was supported by the NASA URETI. J.-Y.H. thanks Dr. S. Chen for making the STM tips, and Prof. Z. F. Ren for providing the CVD nanotubes.

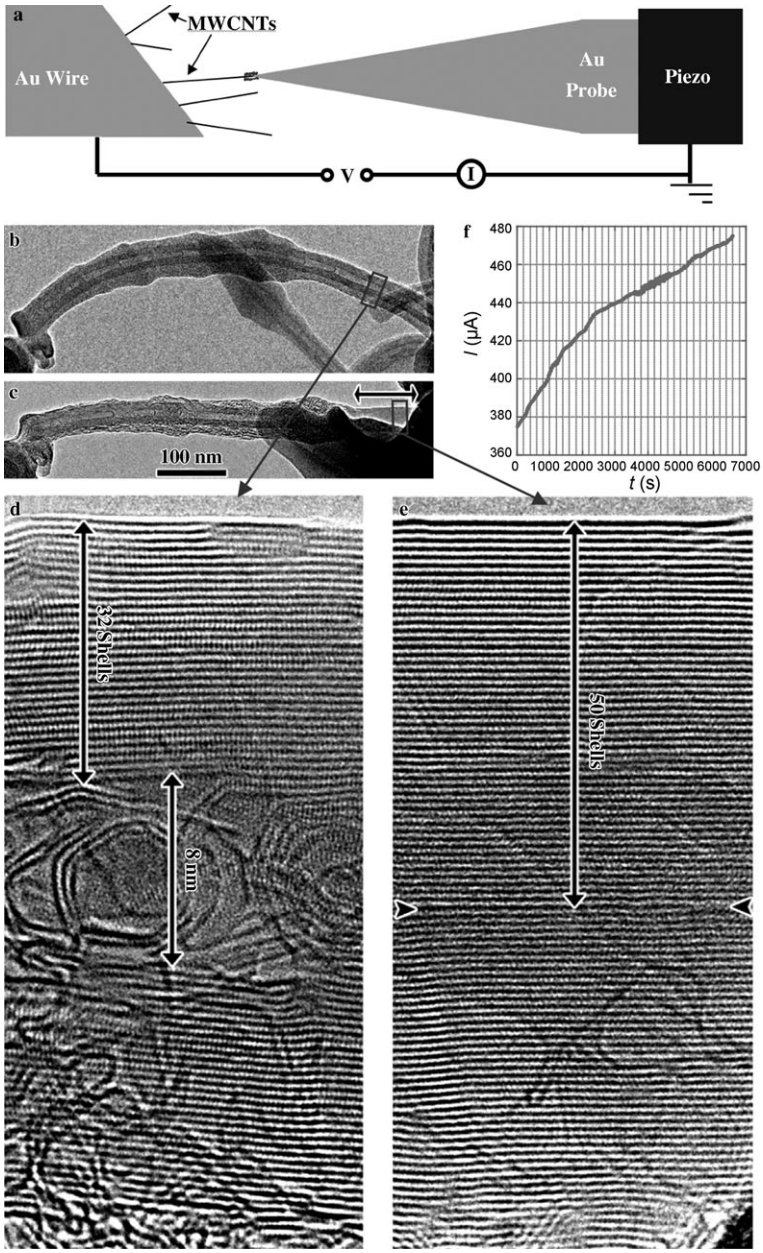

Figure 1. Thickening of a MWCNT through a layer-by-layer self-templated growth mechanism. a) The experimental setup. Individual MWCNTs was connected to the STM tip by electron-beam deposition of amorphous carbon. b) The initial MWCNT. c) The same nanotube as shown in (b) after electric breakdown. An arrow points out the location where electric breakdown occurred. d, e) Magnification of the framed regions in (b) and (c), respectively. The number of walls was increased from 32 (d) to 50 (e) after Joule heating the nanotube for about two hours at a constant bias voltage of 2.3 V. Note that the inner diameter of the nanotube (marked by two arrowheads) was reduced from 8 nm to ≈0.34 nm (one (0002) lattice spacing in graphite). f) The current flowing in the nanotube increased continuously with the increasing number of walls. The bias voltage was fixed at 2.3 V.

Figure 2 shows the self-templated growth of a nanotube wall in the inner surface. Initially, an atomic step was nucleated (indicated by arrowheads in Figure 2a) from both the aggregation of adatoms and diffusion of disordered carbon atoms that remained in the hollow of the MWCNT after electric breakdown. The nanotube wall grew toward the two ends of the nanotube (Figure 2b). As the nanotube wall grew towards the left, it impinged on a giant fullerene and reversed its growth direction (Figure 2b and c).

Figure 3 shows the self-templated growth of a nanotube wall along the outer surface of the nanotube. Figure 3a shows the initial clean nanotube surface. After 8 min, an atomic step with a length of about 16 nm was formed epitaxially on the nanotube surface (Figure 3b) due to the aggregation of adatoms and diffusion of disordered carbon residue left on the nanotube surface after the electric breakdown. The atomic step then grew towards the two ends of the nanotube (Figure 3c) until a complete wall was formed. In the mean time, two Frank dislocations climbed back and forth via dislocation climb.

Dislocation climb occurs only at high temperatures ($T > 0.5T_m$, where T_m is the melting temperature) and is driven by diffusion of vacancies and interstitials.[25,28,33,34] The dislocation climb indicated motions of interstitials and vacancies in the MWCNT. We found two types of edge dislocation (Figure 3). One of them (Figure 3a, b, e, f) is a "sandwich type", with the extra graphene plane residing between two neighboring graphene layers, and the other is a "Y type" (Figure 3c, d, g, h) with the extra plane being bonded to one of the neighboring graphene layer.

The atomic step could also be produced by a dislocation glide. Figure 4a shows a Frank dislocation underneath the surface of a nanotube wall. The Frank dislocation glided along a prismatic plane to the surface of the nanotube, creating an atomic step on the nanotube surface. The atomic step then grew towards the right end of the nanotube until a complete wall was developed.

The nucleation of the atomic steps could initiate from different locations in the nanotube surface. Figure 5 shows

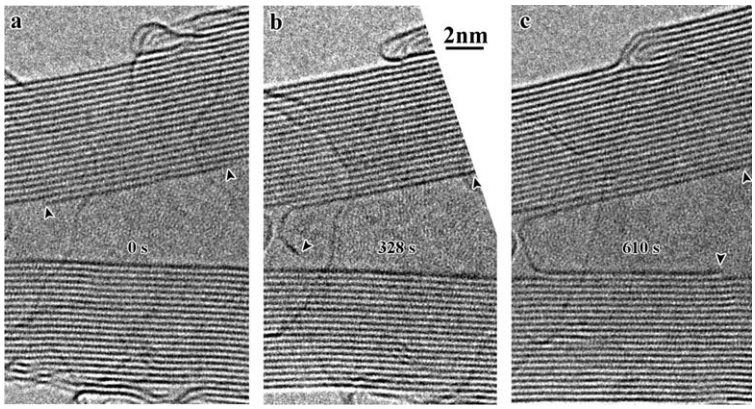

Figure 2. Sequential HRTEM images showing the self-templated growth of a nanotube wall (pointed out by arrowheads) on the inner surface. The time elapsed is marked in each figure. The bias applied to the nanotube was 2 V.

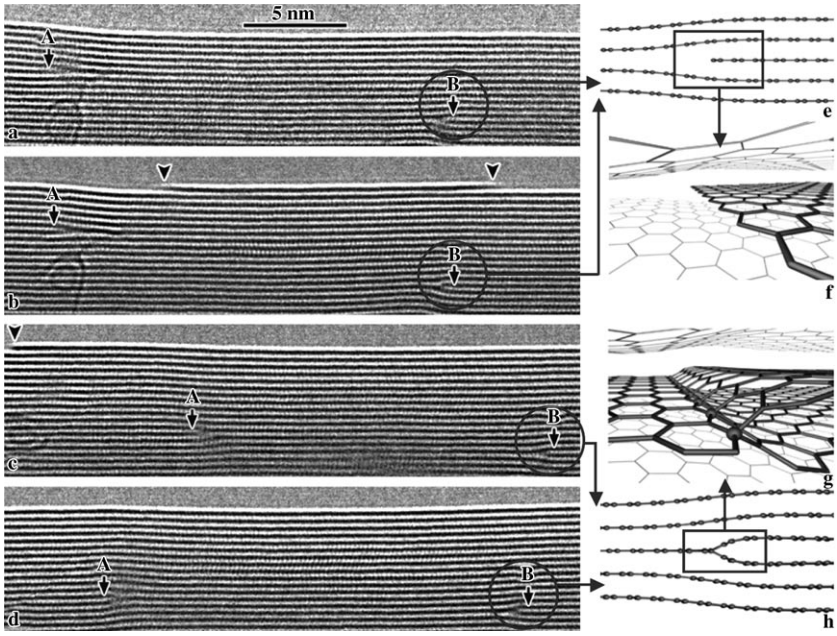

Figure 3. Sequential HRTEM images showing the self-templated growth of a nanotube wall on the outer surface. Arrowheads and arrows point out an atomic step and two Frank dislocations, respectively. a) A clean nanotube surface was produced by electric breakdown. b) An atomic step emerged on the nanotube surface. c) The atomic step in (b) grew towards the two ends of the nanotube. d) A new nanotube wall was grown. e, f) A sandwich-type edge dislocation with an extra graphene plane residing between two neighboring graphene planes. g, h) A Y-type edge dislocation with an extra plane bonded to a neighboring graphene layer.

that two atomic steps grew along opposite directions and then merged to form a complete wall.

The glide of the edge dislocation can be understood by the alternative appearance of the Y-type and sandwich-type dislocations. Figure 6a shows the process of an edge dislocation glide from the center of a four-layer tube to its surface. A Y-type dislocation appears between each glide step. The transformation between sandwich-type and Y-type is illustrated in Figure 6d, where a Y-type and a sandwich-type dislocation are connected by a kink. The motion of the kink along the dislocation line can transfer the dislocation completely to Y-type or sandwich-type. Figure 6c shows that an extra plane is energetically more stable when residing on the tube surface rather than residing between the tube walls.

The carbon source for the self-templated growth was the carbon residue on the nanotube surface. The nucleation and growth of the nanotube walls was attributed to surface and interstitial/vacancy diffusion.[21] The carbon atoms (mostly adatoms) on the nanotube surface were very active and diffused along the nanotube surface. Due to surface diffusion, the adatoms were able to coagulate and form atomic steps, which then grew by further accretion of adatoms on their edges until a complete wall was formed. The activation energy of the surface diffusion is 0.13 eV, which is very low.[21] Theoretical calculation showed that the surface diffusion length λ_{SD} for carbon adatoms varied from 3 to 0.03 μm in the temperature range from 1000 to 2000 K, meaning that the adatoms could travel a long distance along the nanotube surface to reach the edge of the atomic steps.[21] The migration velocity (measured from our in situ experiments) of the atomic steps was generally in the range of $1 \approx 4\ \mathrm{nm\,min^{-1}}$, which is very close to the migration velocity of Frank dislocations. This implies that the diffusion velocity of adatoms on the inner and outer surfaces is close to that of the interstitials and vacancies in the intermediate layers of the nanotubes.

The layer-by-layer growth was not influenced by electromigration, since the growth directions did not depend on the direction of the current. It should be noted that the noncatalytic epitaxial wall growth phenomenon observed here is different from the catalytic growth process.[35,36] In the former, no catalyst was involved, and a temperature higher than 2000 °C was required to drive the carbon-atom diffu-

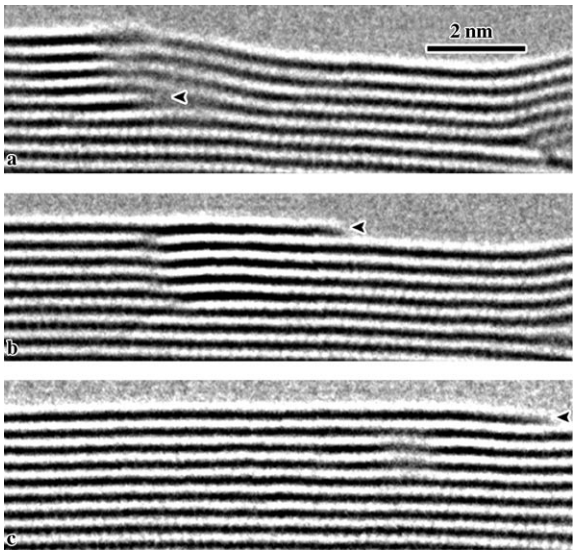

Figure 4. Sequential HRTEM images showing the formation and growth of an atomic step (pointed out by arrowheads) on a nanotube surface. The step was formed by gliding of a Frank dislocation from the interior (a) to the outer surfaces (b) of the nanotube.

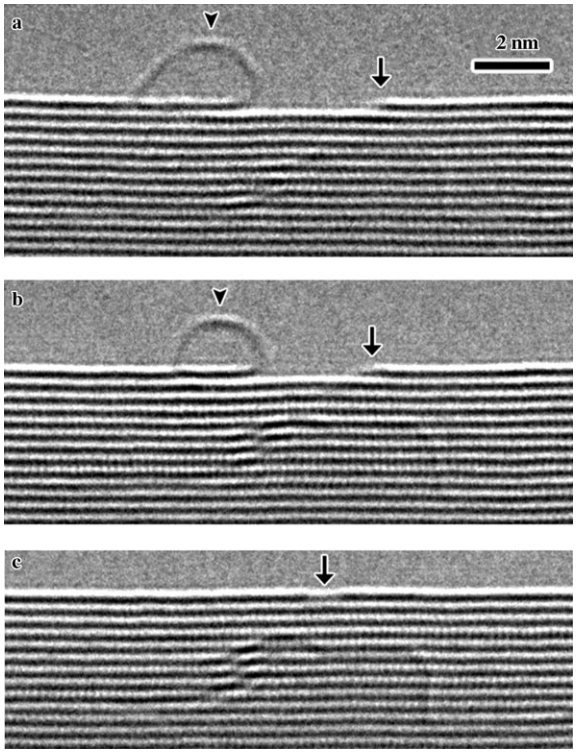

Figure 5. Sequential HRTEM images showing merging of two atomic steps (marked by an arrow and an arrowhead) to form a new nanotube layer. The atomic step on the left of (a) and (b) was rolled up.

sion for the growth of new nanotube walls and anneal the walls to high quality. In the latter, however, the nanotube walls were always precipitated from a catalyst and both fast carbon diffusion across catalyst and efficient carbon-nanotube structure annealing on catalyst surface could be achieved at a relatively low temperature of 600–1000 °C. We did observe catalyst particles in most of the MWCNTs but these catalyst particles always melted and evaporated well before the noncatalytic self-templated wall growth when we ramped up the bias voltages to the nanotubes. The melting and evaporation of the catalysts occurred at much lower temperatures (or applied bias voltages, ≈1–1.5 V) than that required for the noncatalytic wall growth (≈2 V). During the melting or before evaporation of the catalyst particles, precipitation of new nanotube walls from the catalyst particles, similar to that reported previously,[35,36] were frequently observed and such a catalytic wall growth phenomenon is out of the scope of this paper.

The layer-by-layer self-templated growth of nanotube walls is in excellent agreement with the growth model initially proposed by Iijima et al.[16] and later on by others.[19–21] Based on the observation of the presence of incomplete nanotube layers on the nanotube surface, Iijima et al. suggested that the extension and thickening of nanotubes occurred by an island growth of graphite basal planes on the existing nanotube surfaces. Our in situ observation has shown conclusively the validity of this growth model. Our result is also consistent with the model of nanotube growth mediated by surface diffusion.[21] We conclude that individual atomic steps were produced either by the coalescence of adatoms or by the migration of Frank dislocations to the surface of the nanotubes. Surface diffusion drove the atomic steps to extend along the nanotube surface until complete layers were developed.

In summary, we found a noncatalytic layer-by-layer self-templated growth mechanism of carbon nanotube walls when the nanotubes were Joule heated to about 2000 °C inside a HRTEM. The self-templated growth took place on both the inner and the outer surfaces of the nanotubes. In the former, individual atomic steps were first nucleated either from the aggregation of adatoms or from the gliding of Frank dislocations from the interior to the outer surfaces, and the atomic steps then grew epitaxially along the existing nanotube surfaces to form complete nanotube walls. In both cases, the nanotube walls grew at the expense of disordered carbon or adatoms produced by electric breakdown. The self-templated growth results in thickening of the nanotube walls, reduction, or even disappearance of the nanotube hollow, and improvement of conductance. The results prove conclusively that self-templated growth is an important component of the noncatalytic growth of carbon-nanotube walls, and annealing of MWCNTs at high temperatures improves their structure and electronic properties.

Keywords:
carbon nanotubes · noncatalytic growth · conductivity · templates

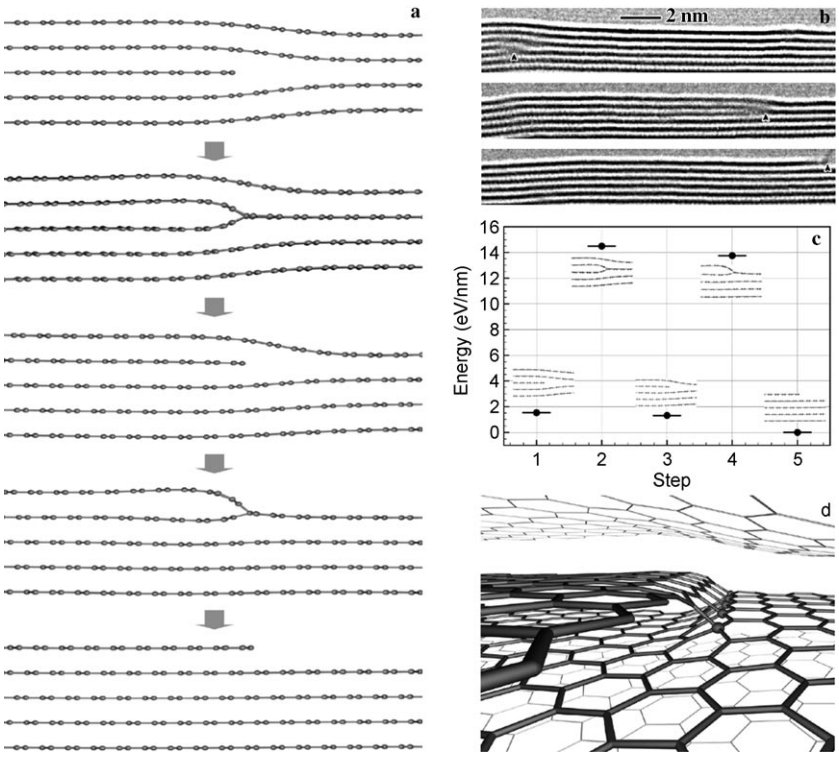

Figure 6. a, b) Theoretical structural models and experimental HRTEM images, respectively, showing the gliding of an edge dislocation from the interior to the outer surface of a nanotube. As the dislocation glided, sandwich-type and Y-type structures appeared alternatively. c) An energy map of the gliding process showing the closer the extra plane to the outer surface the lower the energy. d) An intermediate structure between the sandwich-type and Y-type structures.

[1] S. Iijima, *Nature* **1991**, *354*, 56 – 58.
[2] T. W. Ebbesen, *Carbon Nanotubes: Preparation and Properties* CRC Press, New York, **1997**.
[3] M. S. Dresselhaus, G. Dresselhaus, P. Avouris, *Carbon Nanotubes: Synthesis, Structure, Properties, and Applications* Springer, Heidelberg, Germany, **2001**.
[4] M. J. Treacy, T. W. Ebbesen, J. M. Gibson, *Nature* **1996**, *381*, 678 – 680.
[5] P. Poncharal, Z. L. Wang, D. Ugarte, W. A. de Heer, *Science* **1999**, *283*, 1513 – 1516.
[6] E. W. Wong, P. E. Sheehan, C. M. Lieber, *Science* **1997**, *277*, 1971 – 1975.
[7] B. I. Yakobson, R. E. Smalley, *Am. Sci.* **1997**, *85*, 324 – 337.
[8] A. Javey, J. Guo, Q. Wang, M. Lundstrom, H. J. Dai, *Nature* **2003**, *424*, 654 – 657.
[9] P. G. Collins, A. Zettl, H. Bando, A. Thess, R. E. Smalley, *Science* **1997**, *278*, 100 – 103.
[10] S. Berber, Y. K. Kwon, D. Tomanek, *Phys. Rev. Lett.* **2000**, *84*, 4613 – 4616.
[11] H. Y. Chiu, V. V. Deshpande, H. W. C. Postma, C. N. Lau, C. Miko, L. Forro, M. Bockrath, *Phys. Rev. Lett.* **2005**, *95*, 226101.
[12] C. Dekker, *Phys. Today* **1999**, *52*, 22 – 28.
[13] A. G. Rinzler, J. H. Hafner, P. Nikolaev, L. Lou, S. G. Kim, D. Tomanek, P. Nordlander, D. T. Colbert, R. E. Smalley, *Science* **1995**, *269*, 1550 – 1553.
[14] W. A. de Heer, A. Châtelain, D. Ugarte, *Science* **1995**, *270*, 1179 – 1180.
[15] R. H. Baughman, A. A. Zakhidov, W. A. de Heer, *Science* **2002**, *297*, 787 – 792.
[16] S. Iijima, P. M. Ajayan, T. Ichihashi, *Phys. Rev. Lett.* **1992**, *69*, 3100 – 3103.
[17] D. Zhou, L. Chow, *J. Appl. Phys.* **2003**, *93*, 9972 – 9976.
[18] W. A. de Heer, P. Poncharal, C. Berger, J. Gezo, Z. M. Song, J. Bettini, D. Ugarte, *Science* **2005**, *307*, 907 – 910.
[19] S. Amelinckx, D. Bernaerts, X. B. Zhang, G. Van Tendeloo, J. Van Landuyt, *Science* **1995**, *267*, 1334 – 1338.
[20] X. F. Zhang, X. B. Zhang, G. Van Tendeloo, S. Amelinckx, M. Beeck, J. Van Landuyt, *J. Cryst. Growth* **1993**, *130*, 368 – 382.
[21] O. A. Louchev, *Phys. Status Solidi A* **2002**, *193*, 585 – 596.
[22] P. J. F. Harris, *Carbon* **2007**, *45*, 229 – 239.
[23] J. Y. Huang, S. Chen, Z. Q. Wang, K. Kempa, Y. M. Wang, S. H. Jo, G. Chen, M. S. Dresselhaus, Z. F. Ren, *Nature* **2006**, *439*, 281.
[24] J. Y. Huang, S. Chen, S. H. Jo, Z. Wang, D. X. Han, G. Chen, M. S. Dresselhaus, Z. F. Ren, *Phys. Rev. Lett.* **2005**, *94*, 236802.
[25] J. Y. Huang, S. Chen, Z. F. Ren, Z. Wang, M. Vaziri, Z. Suo, G. Chen, M. S. Dresselhaus, *Phys. Rev. Lett.* **2006**, *97*, 075501.
[26] J. Y. Huang, S. Chen, Z. F. Ren, G. Chen, M. S. Dresselhaus, *Nano. Lett.* **2006**, *6*, 1699 – 1705.
[27] S. Chen, J. Y. Huang, Z. Wang, K. Kempa, G. Chen, Z. F. Ren, *Appl. Phys. Lett.* **2005**, *87*, 263107.
[28] J. Y. Huang, S. Chen, Z. F. Ren, Z. Wang, K. Kempa, M. J. Naughton, G. Chen, M. S. Dresselhaus, *Phys. Rev. Lett.* **2007**, *98*, 185501.
[29] P. G. Collins, H. Hersam, M. Arnold, R. Martel, P. Avouris, *Phys. Rev. Lett.* **2001**, *86*, 3128 – 3131.
[30] B. Bourlon, D. C. Glattli, B. Placais, J. M. Berroir, C. Miko, L. Forro, A. Bachtold, *Phys. Rev. Lett.* **2004**, *92*, 26804.
[31] T. D. Yuzvinsky, W. Mickelson, S. Aloni, S. L. Konsek, A. M. Fennimore, G. E. Begtrup, A. Kis, B. C. Regan, A. Zettl, *Appl. Phys. Lett.* **2005**, *87*, 083103.
[32] T. D. Yuzvinsky, W. Mickelson, S. Aloni, G. E. Begtrup, A. Kis, A. Zettl, *Nano. Lett.* **2006**, *6*, 2718 – 2722.
[33] F. Ding, K. Jiao, M. Q. Wu, B. I. Yakobson, *Phys. Rev. Lett.* **2007**, *98*, 075503.
[34] F. Ding, K. Jiao, Y. Lin, B. I. Yakobson, *Nano. Lett.* **2007**, *7*, 681 – 684.
[35] K. Jensen, W. Mickelson, W. Han, A. Zettl, *Appl. Phys. Lett.* **2005**, *87*, 173107.
[36] J. A. Rodríguez-Manzo, M. Terrones, H. Terrones, H. W. Kroto, L. Sun, F. Banhart, *Nat. Nanotechnol.* **2007**, *2*, 307 – 311.

Received: February 9, 2007
Revised: July 2, 2007
Published online on August 31, 2007

